Vibrational Properties and Vibrational First-Hyperpolarizability of an Octupolar Molecule Based on a Valence-Bond Three Charge-Transfer (VB-3CT) Model

Minhaeng Cho*

Department of Chemistry and Center for Electro & Photo Responsive Molecules, Korea University, Seoul 136−701, KOREA

Received: June 15, 1998; In Final Form: September 2, 1998

Various vibrational characteristics and vibrational first-hyperpolarizability of the octupolar molecule are theoretically described by using a simple four-state (valence-bond and three charge-transfer) model. As the equilibrium value of the bond length alternation coordinate increases by introducing stronger donor and acceptor in the octupolar molecule, (i) the vibrational force constant of the symmetric stretching mode exhibits a nonmonotonic behavior, (ii) that of the asymmetric stretching mode decreases, (iii) IR and Raman intensities of the asymmetric modes increase, and (iv) Raman intensity of the symmetric mode shows a nonmonotonic pattern. Furthermore, it is found that the vibrational hyperpolarizability (β) increases with respect to the equilibrium BLA, and this pattern is qualitatively identical to that of the electronic β.

I. Introduction

Push−pull polyenes consisting of electron donating and accepting groups have been extensively studied over the past decades, and a variety of nonlinear optical (NLO) and vibrational properties were investigated.[1−17] Due to the strong electron vibration coupling, this type of molecule typically exhibits a strong IR transition associated with the concurrent stretching motion of carbon atoms, so-called effective conjugation coordinate[18] or dimerization coordinate,[19] that is defined as the in-phase stretching of all C═C bonds and simultaneous shrinking of all C−C single bonds of the chain. A similar trend can be found in the Schiff bases, charged polyenes, and peptide bond.[20−27] By considering a single effective bond length alternation (BLA) coordinate, the valence-bond charge-transfer (VB-CT) model[12] for the linear push−pull polyene was used to study various vibrational characteristics,[28] such as IR and Raman amplitudes, etc., as well as vibrational contributions to the NLO properties.[28−30] Furthermore, the solvation effect on the vibrational NLO properties was also discussed in ref 28 recently.

Despite that there exist a number of literature sources on the linear push−pull polyenes, there are just a few works on the octupolar molecules having C_3 symmetry.[31−37] Recently, it was suggested that these octupolar molecules have a promising aspect as the alternative to the push−pull polyenes that have a crystallization problem; that is, when the dipolar push−pull polyene forms a crystal, due to the dipole−dipole interaction, they align opposite direction to each other so that the macroscopic hyperpolarizability, $\chi^{(2)}$, becomes rather small.

The molecular orbital calculations and ab initio studies on the NLO properties of the octupolar molecules were presented by Zyss, Silbey, and co-workers and several other groups.[31,32,35,37] To provide a simple physical picture on the NLO responses of the octupolar molecules, the author and co-workers suggested an extended VB-CT model, where one VB configuration and three CT configurations were included to effectively model the electronic structures of the four low-lying electronic states.[33,34] Most of the salient features were found to be qualitatively described by this simple four-state model. Further extension of the model Hamiltonian including three BLA coordinates (see Figure 1) was achieved in ref 34, and the NLO properties of the donor-substituted triphenylmethane dyes were investigated by using the semiempirical calculation method. There, the trend predicted by the VB-3CT model was confirmed.

In this paper, both the vibrational characteristics and vibrational NLO properties of the octupolar molecule are investigated by using the extended VB-3CT model with proper BLA coordinates. The goal of this paper is thus to show that various properties, such as IR and Raman intensities, vibrational frequencies, and vibrational first-hyperpolarizability ($\hat{\beta}^{v}$) are closely related to the molecular structure dictated by the donor or acceptor strengths in a given octupolar molecule. The results obtained here can be used in designing a new type of octupolar molecules having the desired electronic as well as vibrational NLO properties.

II. Vibrational Characteristics and Vibrational First-Hyperpolarizability

From the molecular structure of the octupolar molecules with three polyene branches, it is reasonable to introduce three BLA coordinates as Q_1, Q_2, and Q_3 (see Figure 1 and the figure caption for the definition of Q_1 vibrational coordinate for example). Although there exist a number of intramolecular vibrational modes other than the three BLA coordinates, as usual it is assumed that these effective conjugation modes are most strongly coupled to the electronic degrees of freedom.[12,18,19,28−30] It should be noted that various approximated models including a single BLA coordinate in the model Hamiltonian, such as the VB-CT model for the linear push−pull polyene,[12] SSH model[19] within the mean-field approximation, etc. However, there was no such an attempt to study vibrational properties of the octupolar molecules shown in Figure 1.

Since the bond length difference between a double bond and a single bond in *trans*-1,3,5,7-octatetraene was estimated to be 0.12 Å,[38] each BLA coordinate Q_1, Q_2, and Q_3 can vary from

* Corresponding author. E-mail: mcho@kuccnx.korea.ac.kr.

10.1021/jp982618p CCC: $18.00
Published on Web 05/26/1999

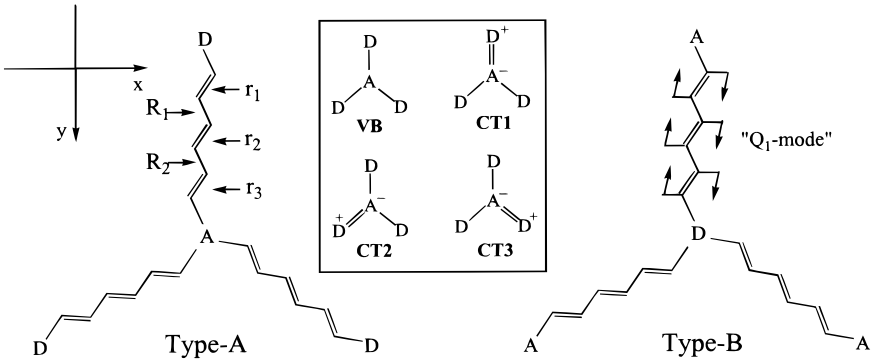

Figure 1. Two types of octupolar molecules are shown. Type-A molecules contain a central acceptor with three peripheral donors connected to the central acceptor via polyene bridges, whereas type-B molecules have a central donor with three acceptors. The valence-bond (VB) and three charge-transfer (CT) configurations are drawn. One of the three BLA coordinates of the three chains, for example the Q_1 mode, associated with the concurrent vibrational motions of the conjugated polyene is shown in this figure. Since the difference between the ideal double and single bond lengths between carbon atoms was estimated to be 0.12 Å, depending on the donor and acceptor, the equilibrium Q_1 value varies from −0.12 to 0.12 Å.

−0.12 to 0.12 Å. Conventionally, the BLA coordinate of the VB configuration is assumed to be −0.12 Å, whereas that of the CT configuration is 0.12 Å.[11,28,30] Then, from the symmetry of the molecular structure, it is reasonable to consider the following model Hamiltonian:

$$H = \begin{pmatrix} H_{VB} & -t & -t & -t \\ -t & H_{CT1} & -T & -T \\ -t & -T & H_{CT2} & -T \\ -t & -T & -T & H_{CT3} \end{pmatrix} \quad (1)$$

where

$$H_{VB} = E^0_{VB} + \sum_{i=1}^{3}\frac{1}{2}k_0(Q_i - Q^0_{i,VB})^2 - \sum_{i=1}^{3}\sum_{j=i+1}^{3} k' Q_i Q_j$$

$$H_{CT1} = E^0_{CT} + \sum_{i=1}^{3}\frac{1}{2}k_0(Q_i - Q^0_{i,CT1})^2 - \sum_{i=1}^{3}\sum_{j=i+1}^{3} k' Q_i Q_j$$

$$H_{CT2} = E^0_{CT} + \sum_{i=1}^{3}\frac{1}{2}k_0(Q_i - Q^0_{i,CT2})^2 - \sum_{i=1}^{3}\sum_{j=i+1}^{3} k' Q_i Q_j$$

$$H_{CT3} = E^0_{CT} + \sum_{i=1}^{3}\frac{1}{2}k_0(Q_i - Q^0_{i,CT3})^2 - \sum_{i=1}^{3}\sum_{j=i+1}^{3} k' Q_i Q_j \quad (2)$$

where k_0 is the force constant of the bond length alternation vibration of an isolated polyene, and it was estimated to be 33.55 eV/Å^2.[12,39] E^0_{VB} and E^0_{CT} are the electronic energies of the VB and CT configurations. Due to the C_3 symmetry, the three CT configurations have the same electronic energy, E^0_{CT}. The mode coupling force constant is denoted as k'. When the octupolar molecule is identical to the fictitious VB configuration (see Figure 1), the equilibrium BLA coordinates are $Q^0_{1,VB} = Q^0_{2,VB} = Q^0_{3,VB} = -0.12$ Å. Those of the CT configurations are $Q^0_{1,CT1} = 0.12$ Å, $Q^0_{2,CT1} = Q^0_{3,CT1} = -0.12$ Å, $Q^0_{2,CT2} = 0.12$ Å, $Q^0_{1,CT2} = Q^0_{3,CT2} = -0.12$ Å, $Q^0_{3,CT3} = 0.12$ Å, and $Q^0_{1,CT3} = Q^0_{2,CT3} = -0.12$ Å, respectively. Note that these equilibrium BLA values are associated with those of the isolated chain. For instance, the CT1 configuration of an octupolar molecule consists of a fully charge-transferred chain and two valence-bond chains. Therefore, the equilibrium BLA coordinate of the chain number 1 is identical to that of the CT configuration of an isolated push−pull polyene, which is 0.12 Å. On the other hand, the other two chains in the CT1 configuration of the octupolar molecule have the same equilibrium BLA values of the VB configuration of an isolated push−pull polyene, which are −0.12 Å.

By carrying out the normal-mode analysis, the three normal modes are obtained, and they are a totally symmetric stretching mode (q_S) and 2-fold degenerate asymmetric stretching modes (q_{A1} and q_{A2}), e.g., $q_S = (Q_1 + Q_2 + Q_3)/\sqrt{3}$, $q_{A1} = (-Q_1 + Q_3)/\sqrt{2}$, and $q_{A2} = (-Q_1 + 2Q_2 - Q_3)/\sqrt{6}$. The q_S mode is of A_1' symmetry, whereas q_{A1} and q_{A2} belong to the E' symmetry representation. Also it should be noted that these three modes are to be considered as approximate normal modes projected onto the axes of the three polyene bridges. The corresponding force constants are $k_S = k_0 - 2k'$ and $k_A = k_{A1} = k_{A2} = k_0 + k'$, respectively. One can approximately estimate the coupling force constant k' by comparing the associated IR and Raman fundamental frequencies of a given octupolar molecule.

By using the normal coordinate representation, the diagonal elements of eq 1 can be rewritten as

$$H_{VB} = E_{VB} + \frac{1}{2}k_S(q_S - q^0_{S,VB})^2 + \frac{1}{2}k_A(q_{A1} - q^0_{A1,VB})^2 + \frac{1}{2}k_A(q_{A2} - q^0_{A2,VB})^2$$

$$H_{CT1} = E_{CT} + \frac{1}{2}k_S(q_S - q^0_{S,CT})^2 + \frac{1}{2}k_A(q_{A1} - q^0_{A1,CT1})^2 + \frac{1}{2}k_A(q_{A2} - q^0_{A2,CT1})^2$$

$$H_{CT2} = E_{CT} + \frac{1}{2}k_S(q_S - q^0_{S,CT})^2 + \frac{1}{2}k_A(q_{A1} - q^0_{A1,CT2})^2 + \frac{1}{2}k_A(q_{A2} - q^0_{A2,CT2})^2$$

$$H_{CT3} = E_{CT} + \frac{1}{2}k_S(q_S - q^0_{S,CT})^2 + \frac{1}{2}k_A(q_{A1} - q^0_{A1,CT3})^2 + \frac{1}{2}k_A(q_{A2} - q^0_{A2,CT3})^2 \quad (3)$$

The constant factors appearing in the normal mode transformation are taken into account by the newly defined E_{VB} and E_{CT}. Here, due to the symmetry, $q^0_{S,CT} \equiv q^0_{S,CT1} = q^0_{S,CT2} = q^0_{S,CT3}$. In eqs 3, the corresponding equilibrium values of $q^0_{S,m}$, $q^0_{A1,m}$, and

$q^0_{A2,m}$, are, for m = VB, CT1, CT2, and CT3,

$$q^0_{S,m} = \frac{k_0}{\sqrt{3}k_S}(Q^0_{1,m} + Q^0_{2,m} + Q^0_{3,m})$$

$$q^0_{A1,m} = \frac{k_0}{\sqrt{2}k_A}(-Q^0_{1,m} + Q^0_{3,m})$$

$$q^0_{A2,m} = \frac{k_0}{\sqrt{6}k_A}(-Q^0_{1,m} + 2Q^0_{2,m} - Q^0_{3,m}) \quad (4)$$

To calculate various quantities based on the model Hamiltonian (3), it is convenient to divide eq 1 into two parts as

$$H = H_0 + H' \quad (5)$$

where

$$H' = -k_A \begin{pmatrix} 0 & 0 & 0 & 0 \\ 0 & q^0_{A1,CT1}q_{A1} + q^0_{A2,CT1}q_{A2} & 0 & 0 \\ 0 & 0 & q^0_{A1,CT2}q_{A1} + q^0_{A2,CT2}q_{A2} & 0 \\ 0 & 0 & 0 & q^0_{A1,CT3}q_{A1} + q^0_{A2,CT3}q_{A2} \end{pmatrix} \quad (6)$$

The zeroth-order Hamiltonian, H_0, is the remaining part of eq 3. The eigenstates of H_0 are found to be[33,34]

$$\Psi_g = (1 - 3l)^{1/2}\phi_{VB} + \sum_{j=1}^{3} l^{1/2}\phi_{CT,j}$$

$$\Psi_{e1} = -2^{-1/2}(\phi_{CT,1} - \phi_{CT,3})$$

$$\Psi_{e2} = -\frac{1}{\sqrt{6}}(\phi_{CT,1} - 2\phi_{CT,2} + \phi_{CT,3})$$

$$\Psi_f = (1 - 3m)^{1/2}\phi_{VB} - \sum_{j=1}^{3} m^{1/2}\phi_{CT,j} \quad (7)$$

where

$$l(q_S) \equiv \frac{1}{6} - \frac{V(q_S) - 2T}{6\sqrt{(V(q_S) - 2T)^2 + 12t^2}}$$

$$m(q_S) \equiv \frac{1}{6} + \frac{V(q_S) - 2T}{6\sqrt{(V(q_S) - 2T)^2 + 12t^2}} \quad (8)$$

Here,

$$V(q_S) = E_{CT} - E_{VB} - k_S(q^0_{S,CT} - q^0_{S,VB})q_S + C \quad (9)$$

with

$$C \equiv \frac{1}{2}k_A(q^0_{A1,CT1})^2 + \frac{1}{2}k_A(q^0_{A2,CT1})^2 = \frac{1}{2}k_A(q^0_{A1,CT2})^2 + \frac{1}{2}k_A(q^0_{A2,CT2})^2 = \frac{1}{2}k_A(q^0_{A1,CT3})^2 + \frac{1}{2}k_A(q^0_{A2,CT3})^2$$

Note that the q_S-dependent l determines the weight of the *CT character* in the electronic ground state. From eq 5, the eigenvalues are obtained as

$$E_g = \frac{1}{2}(U - 2T) - \frac{1}{2}[(V - 2T)^2 + 12t^2]^{1/2}$$

$$E_{e1} = E_{e2} = E_{CT} + \frac{1}{2}k_S(q_S - q^0_{S,CT})^2 + \frac{1}{2}k_A(q^2_{A1} + q^2_{A2}) + C + T \quad (10)$$

$$E_f = \frac{1}{2}(U - 2T) + \frac{1}{2}[(V - 2T)^2 + 12t^2]^{1/2}$$

where

$$U(q_S) = E_{CT} + E_{VB} + \frac{1}{2}k_S[(q_S - q^0_{S,VB})^2 + (q_S - q^0_{S,CT})^2] + k_A(q^2_{A1} + q^2_{A2}) + C$$

By using the eigenstates of the zero-order Hamiltonian and based on the molecular coordinate system drawn in Figure 1, the transition and permanent dipole moments were obtained as[34]

$$\mathbf{M}_{g,e1} = -\frac{l^{1/2}\mu}{2\sqrt{2}}(\sqrt{3},3,0)$$

$$\mathbf{M}_{g,e2} = \frac{3l^{1/2}\mu}{2\sqrt{6}}(\sqrt{3},-1,0)$$

$$\mathbf{M}_{e1,e2} = \frac{\mu}{4\sqrt{3}}(\sqrt{3},3,0)$$

$$\mathbf{M}_{e1} = -\frac{\mu}{4}(\sqrt{3},-1,0)$$

$$\mathbf{M}_{e2} = \frac{\mu}{4}(\sqrt{3},-1,0) \quad (11)$$

Here, $\mathbf{M}_{\alpha,\beta}$ denotes the transition dipole moment between $|\alpha\rangle$ and $|\beta\rangle$ and $\mathbf{M}_\alpha$ is the permanent dipole moment of the $|\alpha\rangle$ state. μ denotes the magnitude of the dipole moment of a given CT configuration. As discussed in ref 33, the permanent dipole moments of the ground and nondegenerate excited state $|f\rangle$ vanish, and also the transition dipole moment between $|g\rangle$ and $|f\rangle$ is zero. Although eqs 11 look identical to eqs 5 in ref 34, since the model Hamiltonian considered in this paper is an extension of that in ref 34, the definition of the CT character l given in eq 8 differs from that in ref 34.

A. Relationship between the Equilibrium BLA Coordinate Q^{eq} and the CT Character, l. Before we present the results on the vibrational characteristics of the octupolar molecule, it would be useful to provide a brief discussion on the connection between the equilibrium BLA coordinate ($Q^{eq} = Q^{eq}_1 = Q^{eq}_2 = Q^{eq}_3$) of each polyene branch and the equilibrium coordinate, q^{eq}_S, of the symmetric stretching mode. From the analytic expressions in eqs 10, one can obtain the self-consistent relationship between the equilibrium BLA coordinate Q^{eq} and the CT character l, as

$$Q^{eq} = \frac{1}{\sqrt{3}}[q^0_{S,VB} - 3(q^0_{S,VB} - q^0_{S,CT})l^{eq}] \quad (12)$$

where l^{eq} is the CT character at the ground-state potential minimum. By self-consistently solving eq 12 with the definition of $l(q_S)$ in eq 8, Q^{eq} can be evaluated for a given set of

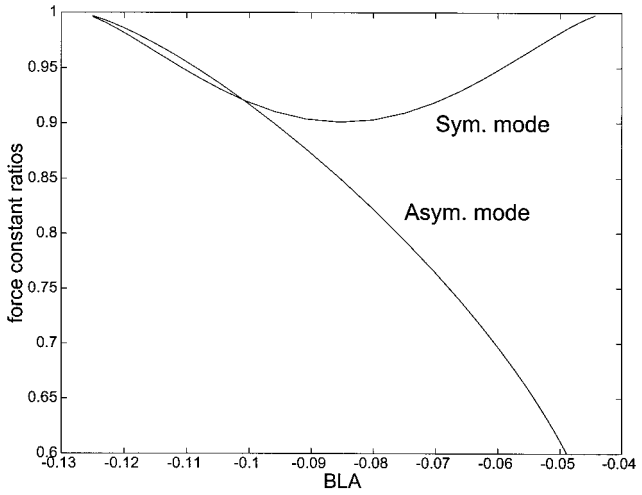

Figure 2. Ratios of the force constants, K_S/k_S and K_A/k_A, are plotted with respect to the equilibrium BLA. Here, the two transfer integrals are assumed to be $t = 1.0$ eV and $T = 0.8$ eV (the general trends are not altered by changes of the two transfer integrals). The force constant k_0 of the linear polyene was estimated to be 33.55 eV/Å^2.[12,39] The coupling force constant is assumed as $k' = 1$ eV/Å^2.

parameters. For given values of the BLA coordinates of the VB and CT configurations discussed above, the above relationship can be simplified as $Q^{eq} = (0.24l^{eq} - 0.12)k_0/k_S$ Å. Despite the existence of the additional term, H', in eq 6, it does not affect to the above calculation since the equilibrium values of the two asymmetric coordinates are all zeroes. From now on, we shall discuss various quantities as functions of the equilibrium BLA coordinate Q^{eq}, which is also proportional to the CT character of the electronic ground state.

Here it should be noted that, if the coupling force constant k' is much smaller than k_0, the equilibrium BLA coordinate in the octupolar molecule could vary from -0.12 to -0.04 Å due to the symmetry. As the donor strength in type-A octupolar molecules increases, the ground-state charge distribution more closely resembles the linear combination of the three CT configurations, and then Q^{eq} approaches to -0.04 Å.

B. Vibrational Force Constant vs Q^{eq}. By using the model Hamiltonian (5), it is possible to obtain the vibrational force constants as functions of Q^{eq}. From the ground-state eigenvalue given in eq 10, the force constant of the q_S mode is found to be

$$K_S = k_S - k_S^2(q_{S,VB}^0 - q_{S,CT}^0)^2 \frac{6t^2}{[(V^{eq} - 2T)^2 + 12t^2]^{3/2}} \quad (13)$$

where V^{eq} is defined in eq 9 at the equilibrium geometry. To calculate the force constant of the asymmetric mode, it was necessary to consider the second-order perturbation correction to the ground-state energy. Second, the force constant of the doubly degenerate asymmetric stretching mode is

$$K_A = k_A - \frac{l^{eq}k_A^2}{E_{e1}^{eq} - E_g^{eq}}(q_{A1,CT1}^0 - q_{A1,CT3}^0)^2$$

$$= k_A - \frac{l^{eq}k_A^2}{3(E_{e2}^{eq} - E_g^{eq})}(q_{A2,CT1}^0 - 2q_{A2,CT2}^0 + q_{A2,CT3}^0)^2 \quad (14)$$

In Figure 2, the above two force constants, K_S and K_A, are plotted with respect to Q^{eq}. As the donor (acceptor) strength increases in type-A(B) molecules, the symmetric and asymmetric modes exhibit different patterns. The symmetric stretching mode force constant shows a nonmonotonic behavior with respect to the CT character of the ground state. In contrast, the force constant of the asymmetric stretching modes decreases monotonically as the CT character increases. Note that the q_S mode is Raman active but IR inactive so that the Raman spectra of a series of octupolar molecules having a common skeleton can be studied to test this theoretical prediction. Likewise, the IR spectra would reveal the frequency red shift of the degenerate asymmetric modes.

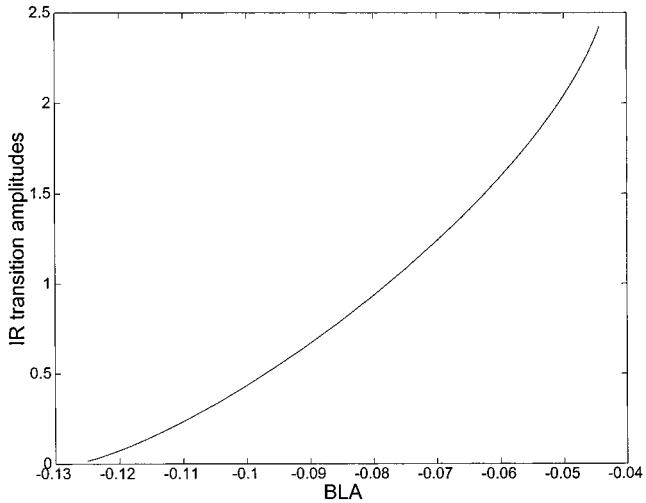

Figure 3. IR transition amplitude, $|(\partial\mu/\partial q_{A1})_{eq}|$, is plotted with respect to the equilibrium BLA. Here the absolute magnitude of the dipole moment of a CT configuration, μ, is assumed to be unity.

C. IR intensity vs Q^{eq}. The IR intensity of a given mode is proportional to $|(\partial\mu/\partial q)_{eq}|^2$. By using the first-order perturbative wave function, we find that the two IR transition amplitudes are given as

$$\left(\frac{\partial\mu}{\partial q_{A1}}\right)_{eq} = -\frac{\sqrt{2l^{eq}}k_A}{E_{e1}^{eq} - E_g^{eq}}(q_{A1,CT1}^0 - q_{A1,CT3}^0)\mathbf{M}_{g,e1}$$

$$\left(\frac{\partial\mu}{\partial q_{A2}}\right)_{eq} = -\frac{2\sqrt{l^{eq}}k_A}{\sqrt{6}(E_{e2}^{eq} - E_g^{eq})}(q_{A2,CT1}^0 - 2q_{A2,CT1}^0 + q_{A2,CT3}^0)\mathbf{M}_{g,e2} \quad (15)$$

Since the two modes, q_{A1} and q_{A2}, are degenerate, the two IR transition amplitude vectors in eq 15 are orthogonal to each other. This can be proved by noting that $\mathbf{M}_{g,e1}\cdot\mathbf{M}_{g,e2} = 0$. Also, the absolute magnitudes of the two IR transition amplitudes are identical, $|(\partial\mu/\partial q_{A1})_{eq}| = |(\partial\mu/\partial q_{A2})_{eq}|$, and it is plotted in Figure 3 as a function of Q^{eq}. It is interesting to note that the IR amplitudes of the two asymmetric modes increase as Q^{eq} or donor (acceptor) strength in the type-A(B) molecules increases.

D. Raman Intensity vs Q^{eq}. The Raman transition amplitude of a given mode is proportional to the Herzberg−Teller term, $(\partial\alpha/\partial q)_{eq}$. To calculate the Raman transition amplitude, one should apply the perturbation approach to not only the ground state but also the 2-fold degenerate excited states. Since the two zero-order states, $|e1\rangle$ and $|e2\rangle$, are degenerate, the correct first-order eigenstates should be obtained by solving the following secular equation:

$$\begin{vmatrix} \langle\Psi_{e1}|H'|\Psi_{e1}\rangle - E & \langle\Psi_{e1}|H'|\Psi_{e2}\rangle \\ \langle\Psi_{e2}|H'|\Psi_{e1}\rangle & \langle\Psi_{e2}|H'|\Psi_{e2}\rangle - E \end{vmatrix} = 0 \quad (16)$$

where the zero-order eigenstates were given in eqs 7.

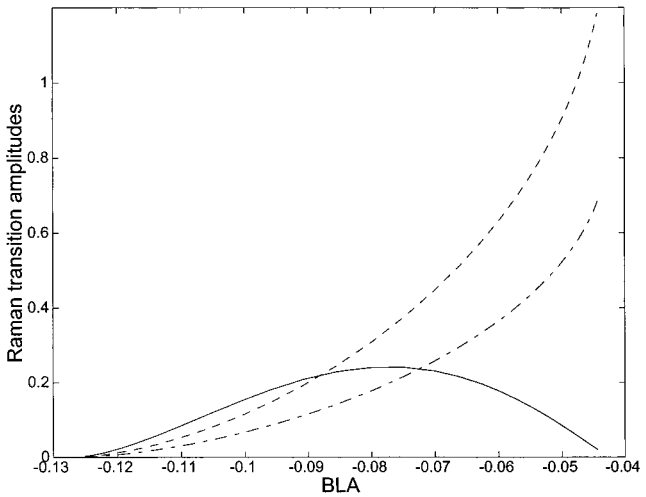

Figure 4. Raman transition amplitudes, $|(\partial\tilde{\alpha}_{yy}/\partial q_S)_{eq}|$, $|(\partial\tilde{\alpha}_{yy}/\partial q_{A1})_{eq}|$, and $|(\partial\tilde{\alpha}_{yy}/\partial q_{A2})_{eq}|$, are shown as solid, dashed, and dash−dotted curves.

From the model Hamiltonian (5) with the correct first-order eigenstates for the excited states, we find

$$\left(\frac{\partial\tilde{\alpha}}{\partial q_S}\right)_{eq} = -\frac{2k_S(q^0_{S,VB}-q^0_{S,CT})t^2}{l^{eq}[(V^{eq}-2T)^2+12t^2]^{3/2}(E^{eq}_{e1}-E^{eq}_{g})}\times (\mathbf{M}_{g,e1}\otimes\mathbf{M}_{g,e1}+\mathbf{M}_{g,e2}\otimes\mathbf{M}_{g,e2}) - \left\{1+\frac{V^{eq}-2T}{[(V^{eq}-2T)^2+12t^2]^{1/2}}\right\}\frac{k_S(q^0_{S,VB}-q^0_{S,CT})}{2(E^{eq}_{e1}-E^{eq}_{g})^2}\times (\mathbf{M}_{g,e1}\otimes\mathbf{M}_{g,e1}+\mathbf{M}_{g,e2}\otimes\mathbf{M}_{g,e2})$$

$$\left(\frac{\partial\tilde{\alpha}}{\partial q_{A1}}\right)_{eq} = -\frac{\sqrt{2l^{eq}}k_A(q^0_{A1,CT1}-q^0_{A1,CT3})}{(E^{eq}_{e1}-E^{eq}_{g})^2}\times (\mathbf{M}_{g,e1}\otimes\mathbf{M}_{e1}+\mathbf{M}_{g,e2}\otimes\mathbf{M}_{e1,e2}) + \frac{k_A(q^0_{A1,CT1}-q^0_{A1,CT3})}{\sqrt{3}(E^{eq}_{e1}-E^{eq}_{g})^2}(\mathbf{M}_{g,e1}\otimes\mathbf{M}_{g,e2})$$

$$\left(\frac{\partial\tilde{\alpha}}{\partial q_{A2}}\right)_{eq} = -\frac{2\sqrt{l^{eq}}k_A(q^0_{A2,CT1}-2q^0_{A2,CT2}+q^0_{A2,CT3})}{\sqrt{6}(E^{eq}_{e1}-E^{eq}_{g})^2}\times (\mathbf{M}_{g,e1}\otimes\mathbf{M}_{e1,e2}+\mathbf{M}_{g,e2}\otimes\mathbf{M}_{e2}) + \frac{k_A(q^0_{A2,CT1}+q^0_{A2,CT3})}{2(E^{eq}_{e1}-E^{eq}_{g})^2}(\mathbf{M}_{g,e1}\otimes\mathbf{M}_{g,e1}) + \frac{k_A(q^0_{A2,CT1}+4q^0_{A2,CT2}+q^0_{A2,CT3})}{6(E^{eq}_{e1}-E^{eq}_{g})^2}(\mathbf{M}_{g,e2}\otimes\mathbf{M}_{g,e2}) \quad (17)$$

In eqs 17, the tilde over α means that $\tilde{\alpha}$ is the second rank tensor, and $\otimes$ is the tensor product. In Figure 4, the absolute values of these Raman transition amplitudes are plotted with respect to Q^{eq}. The Raman intensity of the 2-fold degenerate asymmetric stretching modes is expected to increase as the CT character of the ground state increases by introducing strong donor (or acceptor) in the type-A(B) octupolar molecule. On the other hand, the symmetric stretching mode shows a nonmonotonic pattern.

From the results in eqs 17, we find that, for the q_S mode,

$$\left(\frac{\partial\tilde{\alpha}_{xx}}{\partial q_S}\right)_{eq} = \left(\frac{\partial\tilde{\alpha}_{yy}}{\partial q_S}\right)_{eq} \quad \text{and} \quad \left(\frac{\partial\tilde{\alpha}_{xy}}{\partial q_S}\right)_{eq} = 0 \qquad (18)$$

These relationships are entirely due to the molecular symmetry, and the electronic polarizability tensor elements were also found to have similar relationships, i.e., $\tilde{\alpha}_{xx} = \tilde{\alpha}_{yy}$ and $\tilde{\alpha}_{xy} = \tilde{\alpha}_{yx} = 0$.[33] However, the Herzberg−Teller terms of the asymmetric modes show different relationships among the corresponding tensor elements as

$$\left(\frac{\partial\tilde{\alpha}_{xx}}{\partial q_{A1}}\right)_{eq} = -\left(\frac{\partial\tilde{\alpha}_{yy}}{\partial q_{A1}}\right)_{eq} = \sqrt{3}\left(\frac{\partial\tilde{\alpha}_{xy}}{\partial q_{A1}}\right)_{eq} \quad \text{and}$$

$$\left(\frac{\partial\tilde{\alpha}_{xx}}{\partial q_{A2}}\right)_{eq} = -\left(\frac{\partial\tilde{\alpha}_{yy}}{\partial q_{A2}}\right)_{eq} = -\frac{1}{\sqrt{3}}\left(\frac{\partial\tilde{\alpha}_{xy}}{\partial q_{A2}}\right)_{eq} \quad (19)$$

We shall use these results to establish the relationships among the vibrational first-hyperpolarizability tensor elements in the next section.

E. Vibrational Hyperpolarizability vs Q^{eq} and Its Comparison with the Electronic Hyperpolarizability. As discussed by Zerbi and co-workers recently, the magnitudes of the electronic hyperpolarizabilities of linear push−pull polyenes are quite similar to those of the vibrational hyperpolarizabilities.[29] This quantitative similarity was also experimentally observed for the octupolar molecules. Although the VB-CT model for the linear push−pull polyene showed that the two quantities, electronic and vibrational hyperpolarizabilities, are quantitatively close to each other due to the strong vibronic couplings, there does not exist any theoretical model describing the same pattern found in the octupolar molecules. Here, we apply the four-state model (VB-3CT model) including the BLA coordinates to investigate the relationship between the electronic and vibrational hyperpolarizabilities.

As discussed and derived by several groups,[29,33,40−42] the vibrational contribution to the first-hyperpolarizability denoted as $\hat{\beta}^v$ is given as

$$\hat{\beta}^v \equiv \frac{1}{4\pi^2c^2\nu^2_{A1}}\left(\frac{\partial\mu}{\partial q_{A1}}\right)_{eq}\otimes\left(\frac{\partial\tilde{\alpha}}{\partial q_{A1}}\right)_{eq} + \frac{1}{4\pi^2c^2\nu^2_{A2}}\left(\frac{\partial\mu}{\partial q_{A2}}\right)_{eq}\otimes\left(\frac{\partial\tilde{\alpha}}{\partial q_{A2}}\right)_{eq} \quad (20)$$

Here, the harmonic contributions were only taken into account. Although three vibrational modes were specifically considered in the present study, $\hat{\beta}^v$ is given by a sum over the two asymmetric mode contributions since the symmetric stretching mode is IR inactive. As can be seen in eq 20, each contribution is a product of the IR and Raman transition amplitudes, which were already obtained in the previous subsections. By using the relationships among the Herzberg−Teller tensor elements given in eqs 18 and 19, we find that $\beta^v_{yyy} = -\beta^v_{xxy} = -\beta^v_{xyx} = -\beta^v_{yxx}$ and $\beta^v_{xxx} = \beta^v_{xyy} = \beta^v_{yxy} = \beta^v_{yyx} = 0$. These relationships among the $\hat{\beta}^v$ tensor elements are precisely identical to those found in the electronic β tensor elements. In Figure 5b, β^v_{yyy} is plotted as a function of Q^{eq}. Note that both the electronic and vibrational β_{yyy}'s monotonically increase.[33,34] It will be very interesting to carry out an experiment to test this theoretical prediction. On the basis of this result, it is suggested that the measurement of $\hat{\beta}^v$ can be of use in designing an optimized octupolar molecule with the large NLO property.

III. Discussion and a Few Concluding Remarks

In this paper, theoretical descriptions of the vibrational properties and vibrational first-hyperpolarizability were presented. By taking into account three effective BLA coordinates representing the vibrational motions of the three polyene bridges in a given octupolar molecule, three normal coordinates were

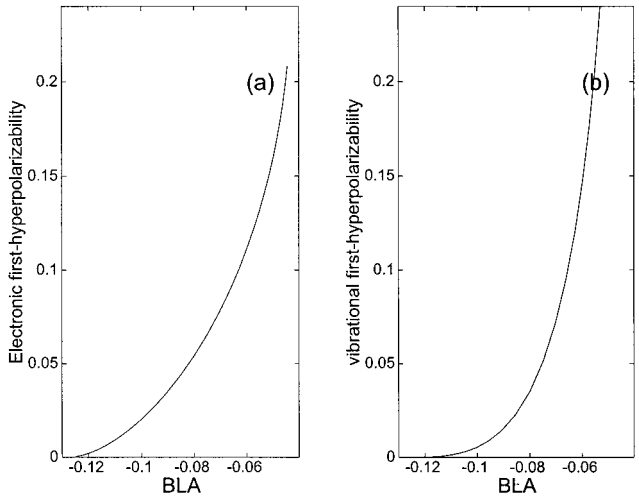

Figure 5. (a) Electronic first-hyperpolarizability (see ref 33 for detailed discussion). (b) Vibrational first-hyperpolarizability, particularly, $(3/K_A)[(\partial\mu_y/\partial q_{A1})_{eq} \otimes (\partial\tilde{\alpha}_{yy}/\partial q_{A1})_{eq} + (\partial\mu_y/\partial q_{A2})_{eq} \otimes (\partial\tilde{\alpha}_{yy}/\partial q_{A2})_{eq}]$ is plotted as a function of the BLA. Note that the two hyperpolarizabilities increases as the BLA increases.

included in the model Hamiltonian. Solving the Hamiltonian by using the standard perturbation theory, we found that various vibrational quantities, such as force constants, IR, and Raman intensities, could be obtained in the analytical forms. Although the perturbation treatment was used in the derivations, it should be emphasized that the results are *exact* because these analytic expressions were evaluated at the ground-state equilibrium geometry; note that, due to the fact that $q_{A1}^{eq} = q_{A2}^{eq} = 0$, the higher-order perturbation correction terms vanish, and this was confirmed by making a comparison of the formal expressions with the numerical calculation results from the model Hamiltonian, eq 2.

Before we close this section, a brief discussion on the merits and shortcomings of the VB-3CT model is presented. As well-known, there exist various levels of theoretical models, such as SSH, PPP, AM1, etc., for describing both the electronic and vibrational properties of polyatomic molecules. These models were proven to be extremely useful in studying electronic as well as vibrational NLO properties of conjugated polyene systems. However, even the simple Huckel model (or SSH model within the mean-field approximation) for the octupolar molecules shown in Figure 1 does not provide analytically exact results for those properties such as electronic NLO properties, vibrational charactersitics (IR and Raman intensities, vibrational frequency shifts, etc.), and vibrational NLO properties. Unlike those models mentioned above, the VB-3CT model is simple enough to solve to obtain the analytic expressions for these quantities. Therefore, it is believed that this model should be of use in describing the general trends of these properties with respect to the structural change of the octupolar molecule by introducing a stronger donor or acceptor. That is to say, without relying on any extensive numerical calculations, one can get a simple physical picture on the structure−function relationship of the octupolar molecules. However, this model does not take into account the electron correlation effects and cannot provide the molecular orbital pictures due to its simplicity. Nevertheless, this model is capable of describing qualitative trends of the NLO properties, and thus it could provide a simple guideline for designing new types of octupolar molecules.

Recently, Bishop, Champagne, and Kirtman presented a work on the relationship between static vibrational and electronic hyperpolarizability of π-conjugated push−pull molecules within the two-state valence-bond charge-transfer model.[43] They used the CPHF/6-31G ab initio calculation method to evaluate the electronic and vibrational polarizabilities and first hyperpolarizabilities of 10 push−pull polyenes. Except for a couple of compounds out of those 10 molecules, both vibrational α and β are found to be quantitatively similar to electronic α and β. As a matter of fact, this similarity between the vibrational and electronic β was also experimentally observed by Zerbi and co-workers. However, the so-called parameter-independent ratios of the vibrational and electronic polarizability and hyperpolarizability were found to dramatically deviate from those values predicted from the two-state VB-CT model. So, they concluded that the assumptions and approximations involved in the VB-CT model are not acceptable for establishing the quantitative relationship between the vibrational and electronic β. Despite their observations, further theoretical investigations involving the electron correlation effect with high-level ab initio methods and experimental confirmation of their results are required to make a more conclusive statement on the validity of the VB-CT model.

Finally, at the end of section II, $\hat{\beta}^v$ in the double harmonic approximation was calculated by using the resultant formal expressions for the IR and Raman amplitudes, and it was found that the increasing pattern of $\hat{\beta}^v$ with respect to the CT character or equilibrum BLA coordiante of the ground state coincides with that of the electronic one, $\hat{\beta}^e$. Therefore, it is confirmed that $\hat{\beta}^v$ is qualitatively similar to $\hat{\beta}^e$. It is hoped that the predicted trends of various quantities discussed in this paper are experimentally confirmed in near future.

Acknowledgment. This work was supported by CRM-KOSEF and Ministry of Education/BSRI-98-3407. The author is thankful for private communications with Prof. D. Bishop on ref 30 and reprints from Prof. B. Champagne on the vibrational NLO properties of linear push−pull polyenes.

References and Notes

(1) Prasad, P. N.; William, D. J. *Introduction to Nonlinear Optical Effects in Molecules and Polymer*; John & Wiley: New York, 1991.
(2) Chemla, D. S.; Zyss, J. *Nonlinear Optical Properties of Organic Molecules and Crystals*; Academic: New York, 1987.
(3) Marder, S. R.; Perry, J. W.; Schaeffer, W. P. *Science* **1989**, *245*, 626.
(4) Samuel, I. D. W.; Ledoux, I.; Dhenaut, C.; Zyss, J.; Fox, H. H.; Schrock, R. R.; Silbey, R. J. *Science* **1994**, *265*, 1070.
(5) Mukamel, S.; Takahashi, A.; Wang, H. X.; Chen, G. *Phys. Rev. Lett.* **1992**, *69*, 65.
(6) Spano, F. C.; Soos, Z. G. *J. Chem. Phys.* **1993**, *99*, 9265.
(7) Kanis, D. R.; Ratner, M. A.; Marks, T. J. *Chem. Rev.* **1994**, *94*, 195. Marks, T. J.; Ratner, M. A. *Angew. Chem., Int. Ed. Engl.* **1995**, *34*, 155.
(8) Meyers, F.; Marder, S. R.; Pierce, B. M.; Bredas, J. L. *J. Am. Chem. Soc*. **1994**, *116*, 10703.
(9) Joffre, M.; Yaron, D.; Silbey, R. J.; Zyss, J. J. *Chem. Phys*. **1992**, *97*, 5607.
(10) Marder, S. R.; Gorman, C. B.; Meyers, F.; Perry, J. W.; Bourhill, G.; Bredas, J. L.; Pierce, B. M. *Science* **1994**, *265*, 632.
(11) Gorman, C. B.; Marder, S. R. *Proc. Natl. Acad. Sci. U.S.A.* **1993**, *90*, 11297.
(12) (a) Lu, D.; Chen, G.; Perry, J. W.; Goddard, W. A., III *J. Am. Chem. Soc.* **1994**, *116*, 10679. (b) Chen, G.; Lu, D.; Goddard, W. A., III *J. Chem. Phys.* **1994**, *101*, 5860.
(13) Chen, G.; Mukamel, S. *J. Chem. Phys.* **1995**, *103*, 9355.
(14) *Material for Nonlinear Optics, Chemical Perspectives*; Marder, S. R., Sohn, J. E., Stucky, G. D., Eds.; ACS Symp. Ser. 455; American Chemical Society: Washington, DC, 1990.
(15) Lyons, M. H. *Materials for Nonlinear and Electrooptics*; J. W. Arrowsmith Ltd.: Bristol, 1989.
(16) Bredas, J. L.; Silbey, R. J. *Conjugated Polymers*; Kluwer: London, 1991.
(17) Prasad, P. N.; Ulrich, D. R. *Nonlinear Optical and Electroactive Polymers*; Plenum: New York, 1988.

(18) Castiglioni, C.; Del Zoppo, M.; Zerbi, G. *J. Raman Spectrosc.* **1993**, *24*, 485.

(19) Fincher, C. R., Jr.; Ozaki, M.; Heeger, A. J.; MacDiarmid, A. G. *Phys. Rev. B* **1979**, *19*, 4140. Heeger, A. J.; Kivelson, S.; Schrieffer, J. R.; Su, W.-P. *Rev. Mod. Phys.* **1998**, *60*, 781.

(20) Harada, I.; Furukawa, Y.; Tasumi, M.; Shirakawa, H.; Ikeda, S. *J. Chem. Phys.* **1980**, *73*, 4746.

(21) Piaggio, P.; Dellepiane, D.; Piseri, L.; Tubino, R.; Taliani, C. *Solid State Commun*. **1984**, *50*, 947.

(22) Lussier, L. S.; Sandorfy, C.; Le-Thanh, L.; Vocelle, D. *J. Phys. Chem.* **1987**, *91*, 2282.

(23) Masuda, S.; Torii, H.; Tasumi, M. *J. Phys. Chem.* **1996**, *100*, 15335.

(24) Yamabe, T.; Akagi, K.; Tanabe, Y.; Fukui, K.; Shirakawa, H. *J. Phys. Chem.* **1982**, *86*, 2359.

(25) Boudreaux, D. S.; Chance, R. R.; Bredas, J. L.; Silbey, R. J. *Phys. Rev. B* **1983**, *28*, 6927.

(26) Zerbi, G.; Castiglioni, C.; Sala, S.; Gussoni, M. *Synth. Met.* **1987**, *17*, 293.

(27) Torii, H.; Tasumi, M. *J. Phys. Chem. B* **1997**, *101*, 466.

(28) Cho, M. *J. Phys. Chem.* **1998**, *102*, 703.

(29) Castiglioni, C.; Del Zoppo, M.; Zerbi, G. *Phys. Rev. B* **1996**, *53*, 13319. Zuliani, P.; Del Zoppo, M.; Castiglioni, C.; Zerbi, G.; Marder, S. R.; Perry, J. W. *J. Chem. Phys.* **1995**, *103*, 9935.

(30) Kim, H. S.; Cho, M.; Jeon, S. J. *J. Chem. Phys.* **1997**, *107*, 1936.

(31) Zyss, J. *J. Chem. Phys.* **1993**, *98*, 6583. Zyss, J.; Ledoux, I. *Chem. Rev.* **1994**, *94*, 77.

(32) Joffre, M.; Yaron, D.; Silbey, R. J.; Zyss, J. *J. Chem. Phys.* **1992**, *97*, 5607.

(33) Cho, M.; Kim, H. S.; Jeon, S. J. *J. Chem. Phys.* **1998**, *108*, 7114; **1998**, *109*, 11131.

(34) Lee, Y.-K.; Jeon, S.-J.; Cho, M. *J. Am. Chem. Soc.* **1998**, *120*, 10921.

(35) Greve, D. R.; Schougaard, S. B.; Geisler, T.; Petersen, J. C.; Bjørnholm, T. *Adv. Mater.* **1997**, *9*, 1113.

(36) Nalwa, H. S.; Watanabe, T.; Miyata, S. *Adv. Mater.* **1995**, *7*, 754.

(37) Luo, Y.; Cesar, A.; Ågren, H. *Chem. Phys. Lett.* **1996**, *252*, 389.

(38) Baughman, R. H.; Kohler, B. E.; Levy, I. J.; Spangler, C. W. *Synth. Met.* **1985**, *11*, 37.

(39) Rappé, A. K.; Casewit, C. J.; Colwell, K. S.; Goddard, W. A., III; Skiff, W. M. *J. Am. Chem. Soc.* **1992**, *114*, 10024. In this paper, the universal force field calculation was carried out to estimate the force constant in eq 2, which is typical for a CC stretching mode when the BLA coordinate is normalized as $Q_1 = (r_1 - R_1 + r_2 - R_2 + r_3)/\sqrt{5}$.

(40) Bishop, D. M.; Kirtman, B. *J. Chem. Phys.* **1991**, *95*, 2646; **1992**, *97*, 5255. Bishop, D. M. *Int. Rev. Phys. Chem.* **1994**, *13*, 21. Bishop, D. M.; Pipin, J.; Kirtman, B. *J. Chem. Phys.* **1995**, *102*, 6778.

(41) Champagne, B.; Perpete, E. A.; André, J.-M. *J. Chem. Phys.* **1994**, *101*, 10796. Kirtman, B.; Champagne, B.; André, J.-M. *J. Chem. Phys.* **1996**, *104*, 4125.

(42) Lee, J. Y.; Kim, K. S. *J. Chem. Phys.* **1997**, *107*, 6515.

(43) Bishop, D. M.; Champagne, B.; Kirtman, B. *J. Chem. Phys.* **1998**, *109*, 9987.